Comparative studies of thermal and mechanical properties of macrocyclic versus linear polylactide

Elodie Louisy, Gaelle Fontaine, Valérie Gaucher, Fanny Bonnet, Grégory Stoclet

Journal : SmallExtended 289	Article No : 3290	Pages : 21	MS Code : 3290	Dispatch : 1-7-2020

Polymer Bulletin
https://doi.org/10.1007/s00289-020-03290-5

ORIGINAL PAPER

Comparative studies of thermal and mechanical properties of macrocyclic versus linear polylactide

Elodie Louisy[1,2] · Gaëlle Fontaine[1] · Valérie Gaucher[1] · Fanny Bonnet[1] · Grégory Stoclet[1]

Received: 22 January 2020 / Revised: 5 May 2020 / Accepted: 27 June 2020

Abstract

This paper reports the study of the influence of the macrocyclic or linear topology of polylactide (PLA) on its resulting thermal and mechanical properties, when displaying identical molar masses. Even if both macrocyclic and linear PLAs crystallize in the same α phase, the results of the calorimetric study and of the tensile tests show some differences which are directly related to the topology of the polymer. The glass transition temperature of macrocyclic PLA was found to be slightly higher than that of the linear one (56 vs 53 °C) while its melting temperature is lower (165 vs 171 °C). Moreover, the crystallization rate of the macrocyclic PLA is slower than that of the linear PLA. Regarding the tensile tests, it has been observed that the macrocyclic PLA displays an earlier strain-hardening than the linear one when stretched in the rubbery state. These differences were attributed to the fact that the macrocyclic topology involves a more constrained entangled network than its linear analogous and/or that the disentanglement kinetics is faster in linear PLA than in macrocyclic PLA.

Keywords Macrocyclic polylactide · Linear polylactide · Thermal properties · Mechanical properties · Macromolecular network

Electronic supplementary material The online version of this article (https://doi.org/10.1007/s00289-020-03290-5) contains supplementary material, which is available to authorized users.

✉ Fanny Bonnet
fanny.bonnet@univ-lille.fr

✉ Grégory Stoclet
gregory.stoclet@univ-lille.fr

[1] Univ. Lille, CNRS, INRAE, Centrale Lille, UMR 8207 - UMET - Unité Matériaux Et Transformations, 59000 Lille, France

[2] Univ. Lille, CNRS, Centrale Lille, Univ Artois, UMR 8181 - UCCS - Unité de Catalyse Et de Chimie du Solide, 59000 Lille, France

Journal : SmallExtended 289	Article No : 3290	Pages : 21	MS Code : 3290	Dispatch : 1-7-2020

Introduction

Despite the numerous advantages of synthetic petrochemical-based polymers, two major drawbacks are still remaining: the use of non-renewable resources to produce them along with their end-life. In this context, developing petroleum-free and biodegradable materials is of high interest. Thus, polylactide (PLA) is particularly relevant as it derives from 100% renewable natural resources, such as corn or beets, and it is also biocompatible and biodegradable [1–3]. These latter properties have contributed to increase its use in various applications, and particularly in medical fields [4]. Furthermore, even if PLA finds numerous short life-time applications, it tends to be considered for longer life-time purposes as blends [5, 6] or composites [7]. PLA can be synthesized by direct condensation of lactic acid [8] or by ring-opening polymerization (ROP) of lactide [9, 10]. Among ROP methods, coordination-insertion ROP of lactides (LA) monitored by metal-based catalysts is a powerful and versatile technique, allowing access to well-defined high molar mass polymers [8–10].

Isotactic polylactides can be prepared directly by the ROP of optically pure L-LA or D-LA, whereas racemic lactide (*rac*-LA) or meso-lactide (*meso*-LA) will usually give rise to atactic polymers, unless specific catalysts are used, in this case heterotactic or isotactic PLA will be obtained [10]. Isotactic poly(L-LA) is a highly crystalline material with a melting temperature (T_m) of 170 °C which displays good mechanical properties [1] and degrades rather slowly, whereas atactic poly(*rac*-LA) is amorphous and subject to faster degradation [11].

In a previous study, we have reported the synthesis of high molar mass macrocyclic polylactide by polymerization of L-lactide under reactive extrusion conditions with lanthanide trisborohydrides complexes, $Ln(BH_4)_3(THF)_3$ (Ln = La, Sm or Nd), as the catalysts [12]. Various investigations have shown that the cyclic topology of a polymer leads to differences in material properties compared to the linear one, such as increased glass transition temperatures (T_g), smaller hydrodynamic volumes and lower intrinsic viscosities [13–15]. Moreover, both the mass and hydrodynamic volumes are substantially reduced compared to linear counterparts, providing a retarded hydrolytic degradation profile [16, 17]. As polylactide exhibits both biodegradability and biocompatibility, this cyclic topology may provide advantages for a range of biomedical applications, such as novel drug delivery vectors [16, 17] or supramolecular hosts [18].

In a recent paper, Zaldua et al. studied the influence of the topology on the crystallization behavior of PLA [19]. Besides, they found that even if the topology has no effect on the crystal structure, this parameter clearly infers on nucleation and consequently crystallization kinetics. Particularly, cyclic PLA chains nucleate much faster than linear ones while no significant effect is observed regarding the growth rate. They explain these differences by both kinetics and thermodynamics effects, and especially by a faster diffusion capacity of the cyclic chains and a lower density of entanglements in cyclic PLA. However, in their study, authors studied linear and cyclic PLA displaying molar masses around 10,000 g/mol, that is to say close to the mass between entanglements (M_e) of PLA which is known

Journal : SmallExtended 289	Article No : 3290	Pages : 21	MS Code : 3290	Dispatch : 1-7-2020

to be around 6000–9000 g/mol [20–22] and thus below the critical molar mass (M_c) which is considered as the critical molar mass values needed to form entanglements. Consequently, it can be assumed that such materials are un-entangled ones and have a brittle behavior and limited mechanical properties limiting their application fields. In addition, due to the synthesis method they used, *i.e.,* the ring closure, some macrocyles and/or linear chains are present into their cyclic PLA, which can infers on the behavior observed.

In the present work, we synthesized two batches of purely linear and macrocyclic polylactides displaying the same molar masses of ≈30,000 g/mol, in order to study the influence of their topology on the resulting thermal and mechanical properties. These investigations were conducted by DSC analysis, tensile tests as well as WAXS analyses.

Material and methods

Reagents

L-lactide (L-LA), supplied by Purac, was conditioned in small sealed bags under vacuum, stored in a glove box ($O_2 = 0$ ppm & $H_2O = 2$ ppm) and used as received (H_2O content, measured by Karl-Fischer analysis, was found inferior to 5 ppm). The sealed bags were open just before mixing L-lactide with the catalyst in the glove box. $La(BH_4)_3(THF)_3$ was synthesized according to the literature procedure [23].

Toluene was supplied by VWR Chemicals (purity ≥ 99.5%, Analar Normapur) and purified in a MBRAUN SPS-800 solvent system. Non-anhydrous chloroform was supplied by Verbiese (purity of 99% stabilized with ethanol). Diethyl ether was supplied by Honeywell (contains BHT as inhibitor, purity ≥ 99.8%). $CDCl_3$ was supplied by Aldrich (purity of 99.8% of D). THF 99 + %, extra pure (stabilized with BHT) was supplied by Acros Organics.

Synthesis of macrocyclic and linear PLA

Macrocyclic PLA was synthesized according to our previously reported procedure [12]. L-lactide (20 g, 0.139 mol) and $La(BH_4)_3(THF)_3$ (55 mg, 1.39×10^{-4} mol) were weighted and mixed together in a glass bottle in a glove box with a manual stirring, before feeding the extruder. The polymerization was performed in a co-rotating twin screw microextruder, from DSM (Geleen, the Netherlands) under nitrogen at a temperature of 130 °C using a residence time of 80 min, and a screw speed of 100 rpm. The conversion of the reaction was determined by ^{1}H NMR analysis of a sample of polymer in $CDCl_3$ and found to be 85%.

In order to purify the obtained macrocyclic PLA, the sample was cryogenically ground and the residual L-lactide was sublimated under vacuum. The cryogrinding was carried out with a Retsch ZM 200. The samples were cryogenically ground at a speed of 10,000 rpm for 30 s. The cryogenically ground polymer was then introduced in a cold finger sublimator immersed in an oil bath heated to

Journal : SmallExtended 289	Article No : 3290	Pages : 21	MS Code : 3290	Dispatch : 1-7-2020

90 °C in order to sublime the residual monomer. This treatment allowed us to isolate macrocyclic PLA with residual monomer content of 3% ($M_n = 29\ 490$ g mol^{-1}, $Đ = 1.27$). The macrocyclic structure of the obtained PLA was confirmed by performing MALDI-ToF analysis on our sample (Fig. 1 and S4).

Linear PLA was synthesized according to a literature procedure [24]. L-lactide (10 g, 6.94×10^{-2} mol) was introduced in a round bottom flask in a glove box along with 14 mL of toluene, and heat-solubilized at 60 °C. $La(BH_4)_3(THF)_3$ (35 mg, 8.67×10^{-5} mol) was solubilized in 7 mL of toluene in the glove box before being added to the monomer solution. The reaction was conducted at 60 °C for 24 min under stirring, leading to a conversion of 51%. At the end of the reaction, the highly viscous medium was dissolved in non-anhydrous chloroform. An aliquot of the obtained solution was taken and dried under vacuum to determine the conversion by ^{1}H NMR in $CDCl_3$. The PLA in solution in chloroform was then poured in diethyl ether. The precipitated PLA was filtered and dried under vacuum, affording purified PLA with residual monomer content of 2% ($M_n = 29{,}000$ g mol^{-1}, $Đ = 1.38$). The linear structure of the obtained PLA was confirmed by MALDI-ToF analysis. (Fig. 1b).

Films Elaboration was carried out by means of compression molding using a Dargon Press. Compression molding was carried out at 200 °C for 3 min (2 min of melting without pressure and 1 min under a pressure of 50 bars), and then, the samples were cooled by air. Tensile test samples were obtained from these films (about 0.2 mm thick). Particularly, the dumbbell-shaped samples (28 mm of length and 5 mm of width) were obtained by laser cutting using a Trotec's Speedy 400 TM Laser Cutting.

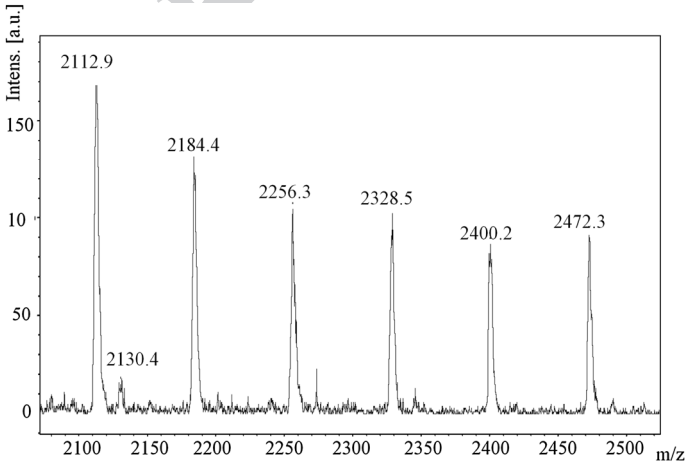

Fig. 1 Maldi-ToF spectrum of purified macrocyclic PLLA synthesized in this study

Journal : SmallExtended 289	Article No : 3290	Pages : 21	MS Code : 3290	Dispatch : 1-7-2020

Characterization techniques

Liquid ^1H NMR ^{1}H NMR spectra of polylactides were recorded on a Bruker Avance 300 MHz instrument at 300 K in $CDCl_3$. The chemical shifts were calibrated using the residual resonances of the solvent. The samples (about 5 to 15 mg) were dissolved in 0.5 mL of $CDCl_3$ in a 5 mm diameter tube. The scan number was set to 32 and the delay (D1) between each scan was set at 4 s. For the spectra relative to the chain-end analysis to confirm the cyclic or linear structure of the polymer, the number of scans of the ^{1}H NMR analysis was set up at 256 scans. The conversion of the reaction was determined by integration of the CH signals of both the residual monomer and the polymer at 5.05 ppm and 5.15 ppm, respectively.

SEC measurements The number–average molar masses (M_n) and dispersities ($Đ = M_w/M_n$) of the polylactides were determined by size exclusion chromatography (SEC) in THF at 40 ºC (1 mL/min) with a triple detection system, equipped with an Alliance Waters e2695, a multiangle light scattering detector (MALS, Wyatt Technology mini DAWN TREOS), and a refractive index detector (Waters 2414). The SEC system was equipped with three Waters Styragel (HT1, HT3 and HT4) columns.

The MALS method was used to determine the absolute molar masses of the cyclic PLLA. The differential refractive index (DRI) increment (dn/dc) value was determined for our macrocyclic PLA and found to be 0.0478 mL g^{-1} in THF at 40 °C [12]. The M_n values of the linear polylactide were determined according to the signal of the refractive index detector with polystyrene standards calibration and Mark–Houwink correction with coefficient 0.58. Samples were prepared by dissolving the product (~ 10 mg) in 4 mL of THF. The solutions were then filtered with 0.45 µm filters.

MALDI-TOF mass spectroscopy measurements Mass spectra were recorded by matrix-assisted laser desorption and ionization time-of-flight (MALDI-TOF) mass spectrometry using a Bruker autoflex III smartbeam mass spectrometer, equipped with the laser that produces pulses at 337 nm using dithranol as a matrix and NaI as cationizing agent. Spectra were recorded in linear mode at an accelerating potential of 20 kV. Samples were prepared by dissolving the polymer in THF at a concentration of 2–5 mg mL^{-1}. A 10 µL aliquot of this solution was mixed with 20 µL of matrix solution and 10 µL of NaI solution (both at 20 mg mL^{-1} in THF). Standards (polystyrenes of known structure, purchased from Polymer Standards Service) were used to calibrate the mass scale.

DSC analysis Thermal analyses were carried out using differential scanning calorimetry (DSC) (TA Instruments Q20). All DSC experiments were performed under a nitrogen atmosphere. The apparatus was calibrated thanks to an indium sample of high purity according to standard procedures. The sample weight was in the range 5–15 mg, and heating and cooling rates were set at 10 °C/min.

Samples were first heated until 200 °C in order to erase thermal history and then cooled down to room temperature before being reheated. Thermal

Journal : SmallExtended 289	Article No : 3290	Pages : 21	MS Code : 3290	Dispatch : 1-7-2020

characteristics were determined from the second heating. Particularly, the glass transition temperature (T_g) is taken at the half of the heat capacity jump and the melting temperature (T_m) at the maximum of the endothermic peak.

The initial degree of crystallinity has been calculated according to the following relation:

$$x_c = \frac{\left(\Delta H_m - \Delta H_{cc}\right)}{\Delta H_m^0}$$

With ΔH_m, the PLA melting enthalpy determined from the endothermic peak area, ΔH_{cc}, the cold crystallization enthalpy determined from the exothermic peak, ΔH_m^0, the standard melting enthalpy of PLA taken equal to 93 J/g [25].

Isothermal crystallization kinetics of both macrocyclic and linear polylactides were also studied for different crystallization temperatures (T_c). Samples were heated up to 200 °C then rapidly cooled down to the desired T_c using a cooling rate of 50 °C/min and held at T_c during 30 min.

Wide Angle X-ray Scattering WAXS experiments were performed using a Xeuss apparatus (Xenos, France) The Cu-K_α radiation used was selected with a curved mirror monochromator. The 2D patterns were recorded on a Pilatus hybrid pixel detector (Dectris, Swiss) and the working distance, around 10 cm, was calibrated using a silver behenate sample. 2D WAXS patterns were azimuthally integrated using the Foxtrot software. Crystallinity degrees of stretched samples have been computed using the method from ref [26].

Tensile tests. Tensile tests were conducted on an Instron 4466 equipment. Two sets of conditions were used:

- tests at 25 °C with an initial strain rate of 10^{-2} s^{-1} in order to determine the Young's modulus in the glassy state.
- tests at 70 °C with an initial strain rate of 4.10^{-2} s^{-1} in order to determine the mechanical behavior of the materials in the rubbery state.

For each set of conditions and each sample type, 5 tests were carried out.

Engineering stress (σ) was calculated as the ratio $\sigma = F/S_0$ where F is the measured force and S_0 the initial cross section of the sample. Engineering strain (ε) is defined as the ratio between the displacement and the initial length of the sample l_0 ($\varepsilon = \frac{\Delta l}{l_0}$).

The Young's modulus (E) was calculated as the slope in the linear region of the engineering stress–strain curve (i.e., between 0 and 0.1%). Finally, strain at break (σ_{break}) was taken as the engineering strain when the sample broke.

Dynamic mechanical analysis Viscoelactic properties were determined by means of DMA experiments. A RSA3 apparatus (TA Instruments, USA) was used in tensile mode. Experiments were carried out on 1-mm-thick samples elaborated using the

Journal : SmallExtended 289	Article No : 3290	Pages : 21	MS Code : 3290	Dispatch : 1-7-2020

same conditions as previously described. Viscoelastic properties, namely E′ and E″, were determined with an applied strain of 0.01% at temperatures varying from 45 to 70 °C on the 0.05–50 Hz frequency range. From these tests, the mastercurves for both linear cyclic PLA were generated using the TA Orchestrator software at a reference temperature $T_0 = 70$ °C.

Results

Synthesis of macrocyclic and linear PLLAs

In order to study the influence of the topology of the PLLA on its thermal and mechanical properties, both macrocyclic and linear polymers displaying the same molar mass were synthesized (Table 1). Macrocyclic PLLA was obtained by reactive extrusion polymerization of L-lactide (in bulk, in the absence of solvent) with lanthanide trisborohyride as the catalyst, according to the procedure reported in our previous study [12]. In order to get materials resistant enough to perform mechanical tests, the lanthanum complex $La(BH_4)_3(THF)_3$ was selected as the catalyst [12], as it gave rise to the formation of macrocycles displaying the highest molar mass of 30,000 g mol^{-1}. The reaction was carried out at 130 °C for 80 min, leading to 85% of conversion.

To ensure the purity of the obtained polymer, the residual monomer was removed AQ1 by sublimation under vacuum in order to preserve the macrocyclic structure of PLLA. This method led to an overall residual L-Lactide content of 3%. The obtaining of macrocyclic PLLA was checked by ^{1}H NMR analysis. MALDI-ToF spectrum of the crude (Figure S4) and purified sample (Fig. 1b) displays a main population relative to macrocyclic polymer and a very minor population relative to HO-PLLA-H, arising from ring-opened macrocycles. Both MALDI-TOF spectra show distributions containing both even-membered and odd-membered oligomers, with peaks separated by 72 Da, indicating the occurrence of transesterification reactions (intramolecular transesterification giving rise to cyclic PLLA). In addition, the macrocyclic PLLA was analyzed by ^{1}H NMR analysis. The signal relative to the chain-end of the residual linear PLLA, HOC*H*Me expected at δ = 4.33 ppm in $CDCl_3$ could be

Table 1 Macrocyclic and linear polylactides synthesized in this study

PLLA	$M_{n\ SEC}$ (g mol^{-1})[c]	$Đ$[c]
Macrocyclic[a]	29,490	1.27
Linear[b]	29,000	1.38

[a]Synthesized by reaction extrusion with $La(BH_4)_3(THF)_3$ as the catalyst. Experimental conditions: m L-LA = 20 g, [L-LA]/[La] = 1000; T = 130 °C; t = 80 min, L-LA non purified, 100 rpm, under nitrogen

[b]Synthesized in toluene with $La(BH_4)_3(THF)_3$ according to the literature procedure.[17]

[c]Determined by SEC (MALLS) in THF at 40 °C, $Đ = M_w/M_n$

Journal : SmallExtended 289	Article No : 3290	Pages : 21	MS Code : 3290	Dispatch : 1-7-2020

observed in the baseline of the ^{1}H spectrum (256 scans) of the crude polymer, but was so low that it was not integrable (Figure S1). Thus, one can conclude that the residual linear fraction in the PLLA was inferior to 1%. SEC analysis of the final polylactide confirmed a molar mass of 29 490 g mol^{-1} and a dispersity of 1.27 (Figure S2).

Regarding the synthesis of the linear polylactide with a molar mass close to the one of the macrocyclic polymer, *i.e.,* about 30,000 g mol^{-1}, a literature procedure involving the same catalyst but in the presence of solvent during the polymerization reaction was used [24]. This reaction procedure is known to afford purely linear dihydroxytelechelic polylactide, [24] whereas our recent study showed that when the same reaction was conducted in bulk conditions (in the absence of solvent), macrocyclic PLLA was obtained [12]. Thus, the polymerization of L-lactide with $La(BH_4)_3(THF)_3$ as the catalyst was conducted in toluene at 60° C for 25 min, leading to 51% of conversion. The polymer was purified by being poured in diethyl ether. SEC analysis of the final polylactide confirmed a molar mass of 29,000 g mol^{-1} and a dispersity of 1.38 (Figure S3). MALDI-ToF analysis confirmed the linear nature of the obtained polylactide (Figure S5).

In order to measure the influence of their topology on their thermal and mechanical properties, both macrocyclic and linear PLAs were subjected to X-ray analysis, DSC analysis as well as tensile tests.

Thermal behavior

Thermal analyses were conducted by differential scanning calorimetry (DSC) on both macrocyclic and linear PLA samples (Fig. 2). The values of the different thermal characteristics are summarized in Table 2. Thermal characteristics of macrocyclic and linear PLAs are measured on second heat.

As shown by the DSC traces depicted in Fig. 2, upon cooling, the macrocyclic PLA exhibits a small crystallization peak at 93 °C (marked by a *) while the linear PLA displays a much more intense one at 98 °C. This indicates that macrocyclic PLA has a slower crystallization kinetic, which may suggest that the macrocyclic structure restrains the molecular mobility.

In the case of the macrocyclic PLA, a glass transition occurs at around 56 °C during the second heating, followed by an exotherm around 106 °C which corresponds to the cold crystallization process. One can also notice the presence of a double

Table 2 Thermal characteristics of macrocyclic and linear PLAs measured on second heat

	Macrocyclic PLA	Linear PLA
T_g (°C)	56 ± 1	53 ± 1
T_{cc} (°C)	106 ± 2	96 ± 2
ΔH_{cc} (J/g)	35 ± 3	4.4 ± 0.5
T_f (°C)	165 ± 2	171 ± 2
ΔH_m (J/g)	42 ± 1	50 ± 1
Initial crystallinity (%)	7 ± 5	49 ± 5

Journal : SmallExtended 289	Article No : 3290	Pages : 21	MS Code : 3290	Dispatch : 1-7-2020

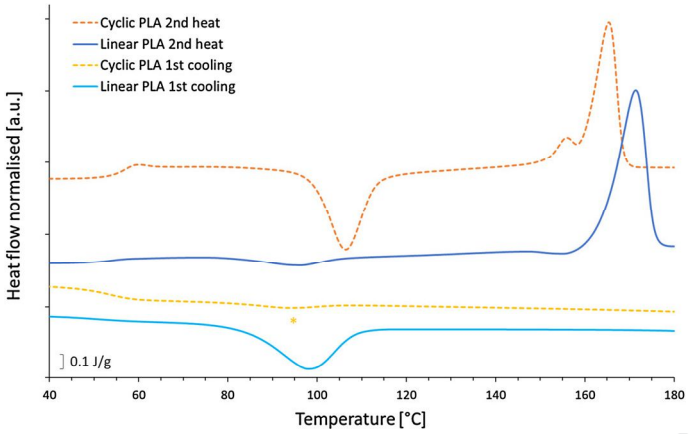

Fig. 2 DSC of macrocyclic and linear PLAs; cooling from the melt at 10 °C/min and subsequent heating at 10 °C/min (endo up)

melting peak at 156 & 165 °C. This phenomenon may be explained by two assumptions: either the existence of two different PLA crystalline structures, displaying different T_f (which was unvalided by X-ray, see below), or a recrystallization melting phenomenon [27, 28], i.e., there is the fusion of a certain amount of the original crystals (at the beginning of the melting), immediately followed by recrystallization into more perfect crystals and final melting of these more perfect crystals.

Regarding the linear PLA, the glass transition is observed at 53 °C, *i.e.,* at a slightly lower temperature than for macrocyclic one, followed by a very small cold crystallization peak at 96 °C and a melting peak at 171 °C.

A 4 °C higher T_g for cyclic PLA as compared to linear PLA has been also reported by Zaldua et al. [19]. The authors explain this difference by the fact that cyclic PLA chains have no chain-ends. As these chains-ends are highly mobile and generate free volume, they are assumed to be responsible of the lower T_g of linear PLA. The latter point cannot alone explain the difference observed regarding the glass transition temperatures. Indeed, the same difference of T_g is observed in the present study and in the one of Zaldua et al. while the chain ends number for linear PLA is about 3 times lower in our case. Consequently, we rather assume that the higher T_g for cyclic PLA depicts a higher rigidity of the chains and/or differences into the macromolecular network due to the cyclic macrostructure rather than to a key role of the chain-ends.

In addition, the higher melting temperature of linear PLA tends to show that thicker and/or more perfect crystals are formed in this material. Regarding the melting peak areas, results show that crystal content induced during the cooling and subsequent heating steps is higher for linear PLA (53% of crystallinity vs 45% for the macrocyclic one), suggesting its stronger ability to crystallize.

In summary, in addition to a slightly higher T_g, macrocyclic PLA seems to have a slower crystallization kinetic than its linear analog, as revealed by the fairly lower amplitude of the crystallization process upon cooling from the melt. Indeed, the

Journal : SmallExtended 289	Article No : 3290	Pages : 21	MS Code : 3290	Dispatch : 1-7-2020

crystallinity degree after cooling at 10 °C/min is about 49% for linear PLA, while it is only 7% for the macrocyclic one. This behavior differs from the one reported in the case of cyclic PLA exhibiting much lower M_n [19], where they observed that cyclic PLA has a faster crystallization kinetics than the linear counterpart.

In order to confirm that macrocyclic PLA has a lower ability to crystallize, a study of the crystallization kinetics was carried out on the two polylactides samples (Fig. 3). Particularly, isothermal crystallizations from the melt state were performed at temperatures varying from 80 to 140 °C with 10 °C steps.

The slower crystallization kinetics of macrocyclic PLA is confirmed by the behaviors observed for the crystallizations ranging from 90 °C to 120 °C where the exotherml related to the crystallization of macrocyclic PLA is systematically broader and starts at longer times. Indeed the crystallization time never exceeds 5 min in the case of linear PLA, while the minimum crystallization time of macrocyclic PLA is 10 min (isothermal at 110 °C).

In addition, no crystallization is observed for both linear and macrocyclic PLAs at $T_c = 140$ °C during the experiment time. At this temperature, crystallization is mainly governed by nucleation aspects (as crystal growth is favored at high temperature) and the higher nucleation ability of cyclic PLA reported by Zaldua et al. [19] does not seem to be observed here. This can be explained by the fact that, as previously mentioned, the molar mass of their material is close to the mass between entanglements of PLA. Consequently, the higher ability to crystallize cyclic PLA may arises from the fact that the chains are very little entangled. In our case, both macrocyclic and linear PLA chains are entangled and as discussed below it could be assumed that the entanglements in the case of cyclic macromolecules are more restrictive from a mobility point of view than the entanglements in the case of linear macromolecules.

In opposition, for $T_c = 80$ °C, an exothermic peak is clearly observed for the linear PLA. By contrast, no crystallization peak is evidenced for the macrocyclic PLA. At

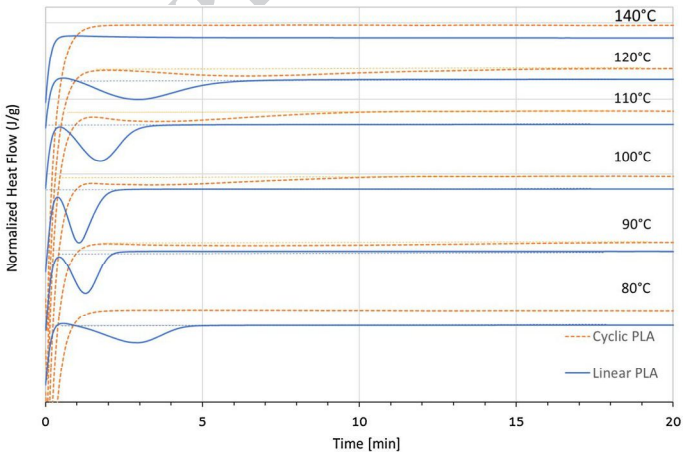

Fig. 3 Crystallization kinetics at different isothermal temperatures of macrocyclic and linear PLA (endo up)

Journal : SmallExtended 289	Article No : 3290	Pages : 21	MS Code : 3290	Dispatch : 1-7-2020

low temperature, it is nucleation which is favored, then crystallization is mainly governed by growth rates aspects. Considering that the two materials have similar molar mass, this difference thus necessarily arises from the different molecular architectures of the PLA and it can be thus conclude that the macrocyclic microstructure involves a slower crystal growth rate due to lower molecular mobility.

Several works have been reported on the crystallization of cyclic and linear polymers. A review of these studies points out that up to now, no unique behavior can be observed. Besides, two opposite trends have been found: the crystallization is slower for cyclic PTHF and PE than for linear analogs (transport and secondary nucleation require higher free energies in cyclic polymers), but faster for cyclic poly(oxyethylene) (POE) and PCL (faster diffusion of cyclic molecules) than for linear analogs [29]. Thus in our case, this behavior could be due to a better mobility of the linear chains compared to the macrocyclic ones, which would allow them to arrange more easily to form the crystal lattice.

Comparing these two studies, we could conclude that linear PLA has a higher ability to crystallize, particularly at low temperatures. Moreover, the macrocyclic structure involves the formation of thinner and/or less perfect crystals.

Structural characterization

Macrocyclic and linear PLAs that have undergone an isotherm at 120 °C were analyzed by means of wide-angle X-ray scattering (WAXS) after recrystallization (Fig. 4). Results indicate that both polymers are semi-crystalline, and the position of the diffraction peaks (13,6°, 14.6°, 16.6° and 22.3°) shows that they crystallize into the α phase [30] in agreement with previously reported results [19].

The crystallinity ratios calculated by XRD are in line with the DSC results, i.e., 50% for the macrocyclic PLA and 59% for the linear one, which confirms that the macrocyclic polymer displays a lower crystallinity degree than its linear analog.

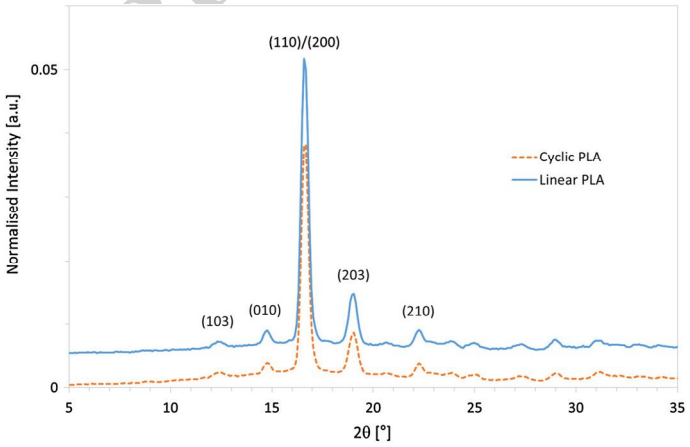

Fig. 4 Diffraction pattern of the PLAs film annealed

Journal : SmallExtended 289	Article No : 3290	Pages : 21	MS Code : 3290	Dispatch : 1-7-2020

Table 3 Summary of tensile tests results at 25 °C

	E (MPa)	σ_{break} (MPa)	ε_{break} (%)
Macrocyclic PLA	2510 ± 98	32 ± 2	1 ± 1
Linear PLA	2408 ± 278	36 ± 7	1.5 ± 1

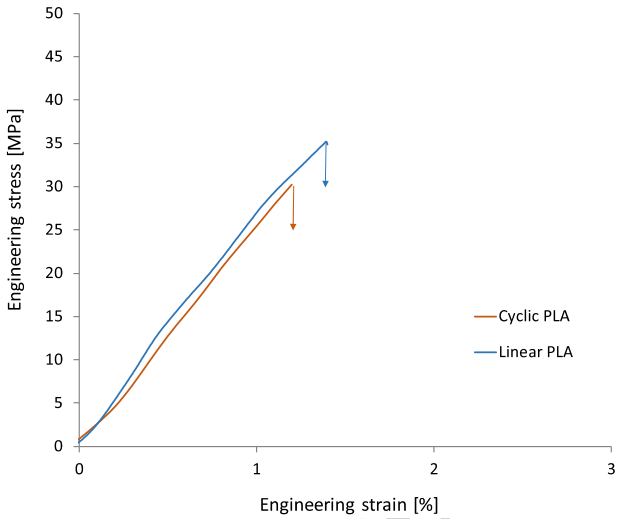

Fig. 5 Engineering stress–strain curves at 25 °C and $\dot{\varepsilon} = 10^{-2}$ s^{-1}

Mechanical study of macrocyclic and linear PLAs

Tensile tests were performed on amorphous films obtained by compression molding. A set of experiments were carried out at 25 °C in order to determine the end-to-use properties of the materials. Mechanical properties are reported in Table 3.

At 25° C (Fig. 5), both materials exhibit a brittle behavior with no sign of plastic deformation. In addition, both materials have roughly the same Young's modulus, around 2.5 GPa, characteristic of an amorphous polymer into its glassy state. Consequently, no main difference can be observed during cold-drawing.

Mechanical properties were also studied in the rubbery state (Fig. 6). The drawing temperature has been chosen so as to be between T_g and T_{cc}, i.e., at sufficiently high temperature to obtain materials in their rubbery state and sufficiently low temperature to prevent any thermally induced crystallization phenomenon.

The mechanical behavior is roughly the same whatever the PLA type and characteristic of an initially amorphous sample drawn in its rubbery state (*e.g.,* PET). Besides, after a viscoelastic deformation stage at low strains, plastic deformation occurs at a similar strain value. Then, for larger deformations, a strain-hardening phenomenon is observed in both cases. The main differences between the two materials are that strain-hardening starts at lower strains for macrocyclic PLA

Journal : SmallExtended 289	Article No : 3290	Pages : 21	MS Code : 3290	Dispatch : 1-7-2020

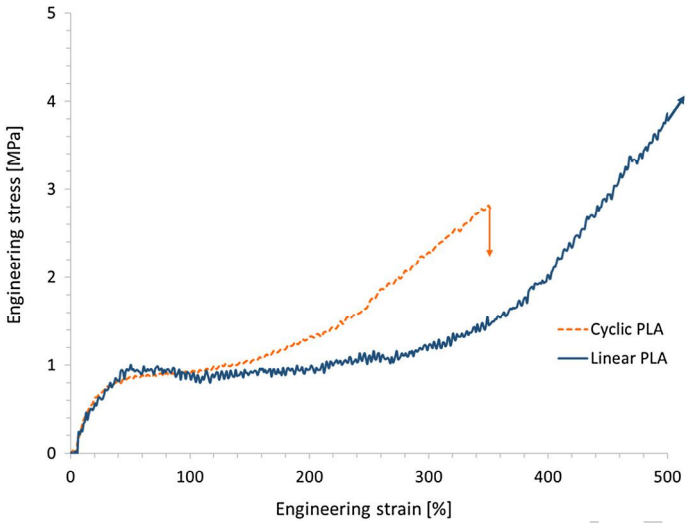

Fig. 6 Engineering stress–strain curves at 70 °C and $\dot{\epsilon} = 10^{-2}\ s^{-1}$

(*i.e.*, 200% for macrocyclic PLA vs 350% for linear PLA). In the case of PLA, strain-hardening is related to the occurrence of a strain-induced crystallization, the beginning of crystallization being governed by the achievement of a critical macromolecular orientation degree. Consequently, it can be assumed that macrocyclic PLA has a better ability to macromolecular orientation upon stretching. Finally, it is also observed that the linear PLA can undergo a very large deformation at break, i.e., > 500% while the one of cyclic PLAs is lower, around 400%.

In order to confirm the occurrence of strain-induced crystallization upon stretching, and in order to assess the influence of the topology on the strain-induced structure, post-mortem WAXS analyses were also performed on drawn samples and comparison of patterns and diffractograms before and after the tensile tests are presented in Figs. 7 and 8. The values of the crystallinity rate calculated by XRD are summarized in Table 4.

Before stretching both linear and macrocyclic PLAs are fully amorphous, as shown in the 2D WAXS images (Fig. 7) and the crystallinity rate (Table 3). After stretching (300% of strain for macrocyclic PLA vs 430% for the linear one), the integrated intensity profiles (Fig. 8) clearly show the presence of crystals into both materials confirming that the occurrence of strain-induced crystallization is at the

Table 4 Crystallinity degree calculated by XRD

	Macrocyclic PLA BT	Macrocyclic PLA AT70	Linear PLA BT	Linear PLA AT70
Crystallinity (%)	0	35 ± 5	0	40 ± 5

BT before traction; AT70: After Traction at 70 °C

Journal : SmallExtended 289	Article No : 3290	Pages : 21	MS Code : 3290	Dispatch : 1-7-2020

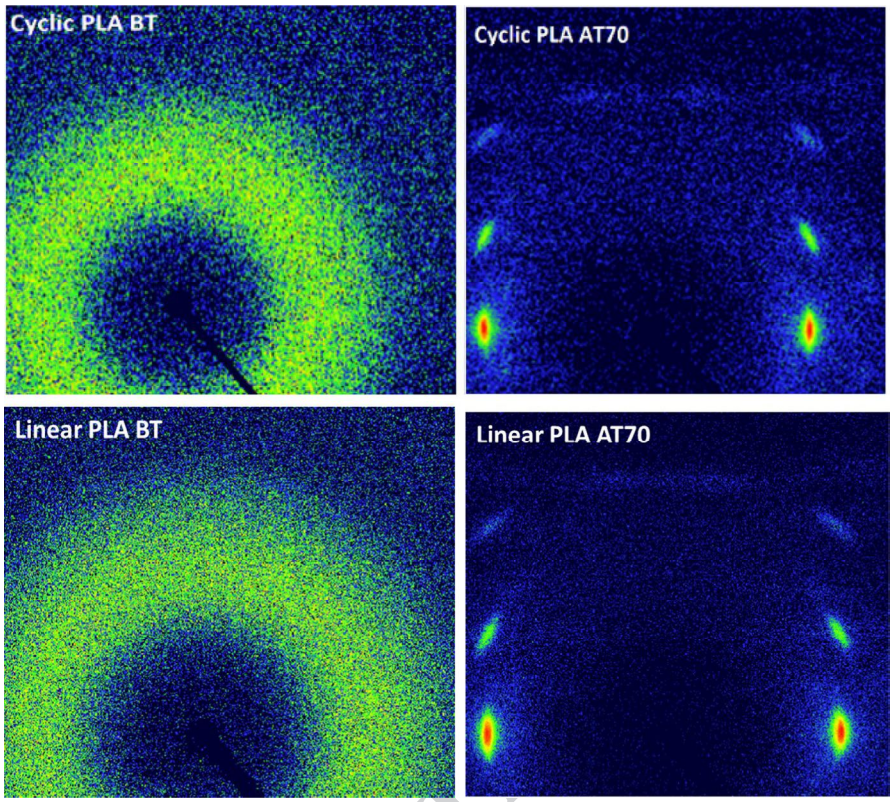

Fig. 7 Diffraction patterns of PLAs before (BT) and after (AT70) tensile tests at 70 °C (the stretching axis is vertical)

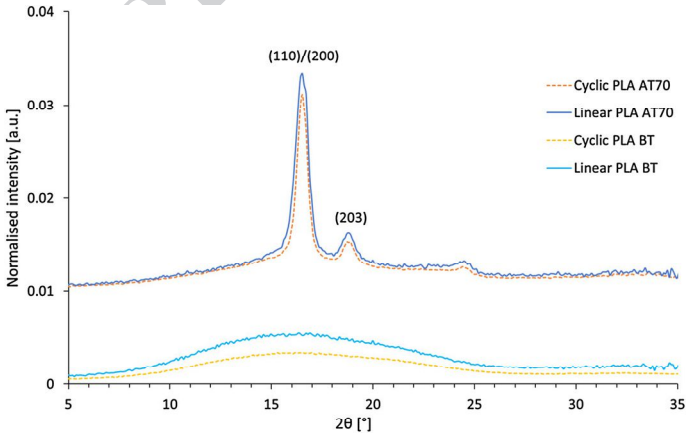

Fig. 8 Diffraction pattern of PLAs before (BT) and after (AT70) tensile tests at 70 °C

Journal : SmallExtended 289	Article No : 3290	Pages : 21	MS Code : 3290	Dispatch : 1-7-2020

origin of the strain-hardening stage observed on the stress–strain curves. The earlier occurrence of strain-induced crystallization for macrocyclic PLA is probably ascribed to a faster increase in the macromolecular orientation upon stretching, as compared to linear PLA.

Moreover, the position of the diffraction peaks shows that it is the α' phase (Fig. 8) which is involved in both cases [31]. Finally, we also note that the crystallinity rates of macrocyclic PLA (35%) is slightly lower than the one of linear PLAs (40%) (Table 3).

Discussion: Entanglement in cyclic and linear structures

The examination of the mechanical behavior in the rubbery state, and in particular the earlier occurrence of the strain-induced crystallization process in the case of macrocyclic PLA, may suggests that the entanglement network of the macrocyclic PLA is more constrained than the one of the linear one. Indeed the occurrence of strain-induced crystallization in PLA could be linked with an achievement of a critical orientation degree of the macromolecules [32]. Consequently, it appears that in macrocyclic PLA, the macromolecules orient faster upon stretching than in linear PLA which tends to show that macrocycles have a slower disentanglement kinetics than the linear chains which favors macromolecular orientation upon stretching explaining the difference in the mechanical behavior observed.

The examination of the viscoelastic properties, especially in the rubbery domain, is known to be a good probe of the macromolecular architecture. Notably, the value of the storage modulus in this region could be directly related to the mass between the entanglements of the polymer according to the following equation:

$$M_e = \frac{\rho RT}{G_N^0}$$

with G_N^0 being the value of the storage modulus G′ measured in plateau modulus (at the minimum of the loss modulus G″), ρ the density of the material at the considered temperature, R the universal gas constant and T the considered temperature in K. In our study, viscoelastic properties were determined in the tensile mode, however, as G′ and E′ are proportional the previous equation can also be applied. Figure 9 depicts the mastercurves obtained for both cyclic and linear PLAs at the reference temperature $T_0 = 70$ °C.

The value of M_e, could be assessed by the determination of E′ in the low frequency region, where the materials are in the rubbery state. Experiments were repeated three times for each material, and the analyses revealed that no differences could be observed regarding the plateau modulus, around 4 MPa, for both macrocyclic and linear PLAs. Consequently, the macrocyclic structure does not infer on the mass between the entanglements of PLA. The only slight difference which can be evidenced from these experiments if that the crossover point between E′ and E″ occurs at a slightly higher frequency ω_c for linear PLA. $1/\omega_c$ could be related to a characteristic relaxation of the material [33] and thus, even if both times are of the

Journal : SmallExtended 289	Article No : 3290	Pages : 21	MS Code : 3290	Dispatch : 1-7-2020

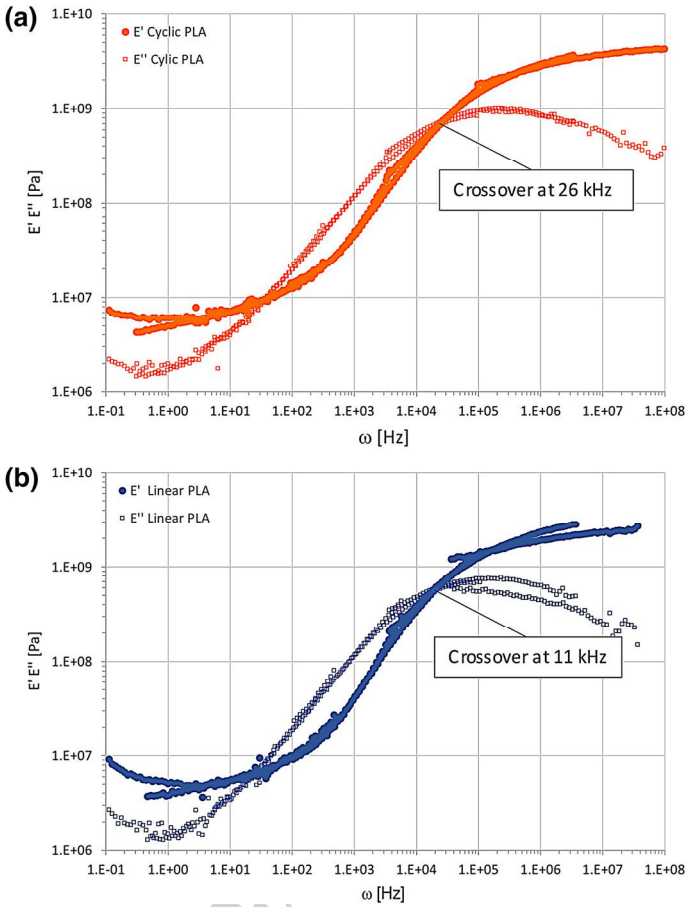

Fig. 9 Storage modulus (E′) and loss modulus (E″) as a function of frequency at $T_0 = 70$ °C for **a** macrocyclic PLA and **b** linear PLA

same order of magnitude, the relaxation time of linear PLA is slightly lower than the one of its macrocyclic analog.

The observation of a rubbery plateau for PLA seems to be in contradiction with the results obtained by Doi et al. in the case of polystyrene (PS) [34]. Indeed in their study where they analyze the viscoelastic behavior of ring PS with various molecular weights, authors never observe a rubbery plateau. However, they nevertheless observe for high molecular weight PS, a deviation to the standard behavior (i.e., Rouse like model). Authors attribute this deviation to the formation of intermolecular interactions such as ring penetrations. The fact that a rubbery plateau is observed in our case for macrocyclic PLA also shows that (i) the macrocycles can also entangle themselves, and (ii) that the entanglement network is more stable in PLA than in PS. This higher stability for PLA should be explained by the differences of Me between PS and PLA. Indeed, considering that PLA and PS exhibit similar values

Journal : SmallExtended 289	Article No : 3290	Pages : 21	MS Code : 3290	Dispatch : 1-7-2020

regarding the chain rigidity [35–37], the Me of PLA is about 4–5 times lower than the one of PS. Consequently, the entanglement network formed by the PLA macrocycle is probably more constrained, i.e., the macromolecules have less mobility.

As a result of this work, and in the same way than what was shown by Doi et al. for PS [34], the macromolecular network understanding seems to be a key point to explain the behavior differences between cyclic polymers and their linear analogues. Besides, it appears that the fact that the molar mass of the material is below or above M_c significantly changes the material behavior. On the one hand, when M_n is below M_c, cyclic PLA displays a faster macromolecular dynamics involving besides a faster crystallization kinetics than its linear counterpart. On the other hand, when the materials are entangled (i.e., when Mn is above Mc as in this study), the crystallization kinetics is slower for macrocyclic PLA and this material has a faster macromolecular orientation rate upon stretching.

The macromolecular network and the concept of entanglement have been deeply studied in the case of linear polymers and are now well understood as depicted in Fig. 10a. On the other hand, entanglements in cyclic polymers as well as the macromolecular organization in the amorphous bulk remain poorly addressed. An attempt of structural representation is schematized in Fig. 10b, and, as can be seen, interpenetration of macrocycles can lead to locally completely locked structures contrary to the case of linear polymer where the chains can disentangle more easily due to fact that they do not form a closed structure and are consequently more labile. Similar locked structures have been also proposed by Submarian et al. in their modeling study of DNA [38]. Still using a numerical approach, threading, i.e., interpenetration, between large cycles has also been proposed by Lee et al. [39] as well as Tsalikis et al. [40].

This representation also allows to understand the lower mobility of macrocyclic chains. Indeed, it clearly appears that the interpenetration of macrocycles could lead to a more constrained network with less mobility degrees. This explains the slower crystallization kinetics observed for macrocyclic PLA. In addition, the presence of these locally locked structures formed by the interpenetration of two macrocycles could be at the origin of the faster macromolecular orientation observed during stretching in the rubbery state as previously discussed. Indeed, due to these constrains the relaxation time of macrocyclic PLA chains is higher than that of linear PLA (see DMA results). Consequently, upon stretching, the macrocyclic PLA chains relax less than the ones of linear PLA and thus orient themselves faster involving an earlier occurrence of strain-induce crystallization.

Conclusion

This study aimed at comparing the behavior between macrocyclic and linear polylactides displaying identical molar masses, allowing to highlight the influence of the polymer topology on its structure and properties. Regarding thermal properties, the glass transition temperature of the macrocyclic PLA is slightly higher than that of the linear one as expected (56 vs. 53 °C) [13-15], while its

Journal : SmallExtended 289	Article No : 3290	Pages : 21	MS Code : 3290	Dispatch : 1-7-2020

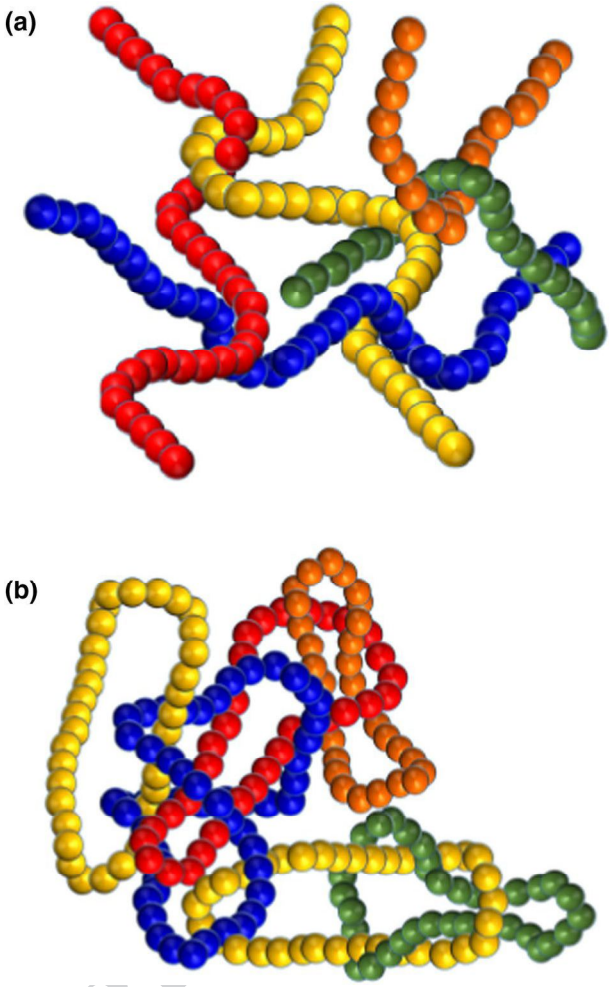

Fig. 10 Schematic representation of the macromolecular networks in the cases of **a** a linear polymer and **b** a cyclic polymer

melting point is lower (165 vs. 171 °C) indicating that the macrocyclic architecture induces the formation of smaller and/or more defective crystals.

Moreover, the crystallization kinetics of PLA is strongly influenced by its topology. Indeed, macrocyclic PLA has a lower crystallinity, *i.e.,* 50% vs 59% for the linear one (XRD) but especially has a slower crystallization kinetics which is ascribed to the fact that the macrocyclic structure restricts the molecular mobility. Tensile tests conducted at 70 °C showed that linear PLA had a much higher deformation capacity than its macrocyclic analog. This is attributed to the more constrained macromolecular network of the macrocyclic PLA and could have some implications regarding its processing. Finally, regarding the strain-induced

Journal : SmallExtended 289	Article No : 3290	Pages : 21	MS Code : 3290	Dispatch : 1-7-2020

structure under tensile tests at 70 °C and the mechanical properties at room temperature, no significant difference between the two materials was evidenced.

Acknowledgements The authors would like to thank Aurélie Malfait for SEC analysis, Dr François Stoffelbach for MALDI-ToF analysis, CNRS and Région Hauts de France for fundings. The project ARCHI-CM, Chevreul Institute (FR 2638), Ministère de l'Enseignement Supérieur et de la Recherche, Région Nord-Pas de Calais and European Regional Development Fund (FEDER) are acknowledged for supporting and funding the SAXS-WAXS laboratory.

References

1. Auras R, Lim L-T, Selke SEM, Tsuji H (2010) Poly(Lactic Acid): Synthesis, structures, properties, processing, and applications. Wiley, Hoboken
2. Jamshidian M, Tehrany EA, Imran M, Jacquot M, Desobry S (2010) Poly-lactic acid: production, applications, nanocomposites, and release studies. Compr Rev Food Sci F 9:552–571. https://doi.org/10.1111/j.1541-4337.2010.00126.x
3. Slomkowski S, Penczek S, Duda A (2014) Polylactides: an overview. Polym Adv Tech 25(5):436–447. https://doi.org/10.1002/pat.3281
4. Pawar RP, Tekale SU, Shisodia SU, Totre JT, Domb AJ (2014) Biomedical applications of poly(lactic acid). Recent Pat Regen Med 4:40–51. https://doi.org/10.2174/2210296504666140402235024
5. Krishnan S, Pandey P, Mohanty S, Nayak SK (2016) Toughening of polylactic acid: an overview of research progress. Polym Plast Technol Eng 55(15):1623–1652. https://doi.org/10.1080/03602559.2015.1098698
6. Murariu M, Dubois P (2016) PLA composites: from production to properties. Adv Drug Deliv Rev 107:17–46. https://doi.org/10.1016/j.addr.2016.04.003
7. Dechy-Cabaret O, Martin-Vaca B, Bourissou D (2004) Controlled ring-opening polymerization of lactide and glycolide. Chem Rev 104(12):6147–6176. https://doi.org/10.1021/cr040002s
8. Jérôme C, Lecomte P (2008) Recent advances in the synthesis of aliphatic polyesters by ring-opening polymerization. Adv Drug Deliv Rev 60(9):1056–1076. https://doi.org/10.1016/j.addr.2008.02.008
9. Dagorne S, Normand M, Kirillov E, Carpentier J-F (2013) Gallium and indium complexes for ring-opening polymerization of cyclic ethers, esters and carbonates. Coord Chem Rev 257(11–12):1869–1886. https://doi.org/10.1016/j.ccr.2013.02.012
10. Carpentier J-F (2010) Discrete metal catalysts for stereoselective ring-opening polymerization of chiral racemic β-Lactones. Macromol Rapid Commun 31(19):1696–1705. https://doi.org/10.1002/marc.201000114
11. Hakkarainen M (2002) Aliphatic polyesters: abiotic and biotic degradation and degradation products. In: Degradable aliphatic polyesters. Adv. Polym. Sci., vol 157. Springer, Berlin, pp 113–138
12. Bonnet F, Stoffelbach F, Fontaine G, Bourbigot S (2015) Continuous cyclo-polymerisation of L-lactide by reactive extrusion using atoxic metal-based catalysts: easy access to well-defined polylactide macrocycles. RSC Adv 5(40):31303–31310. https://doi.org/10.1039/C4RA16634E
13. Roovers J (2002) Chapter 10: organic cyclic polymers. In: Semlyen JA (ed) Cyclic polymers, 2nd edn. Kluwer, Dordrecht, pp 347–383
14. Kricheldorf HR (2010) Cyclic polymers: Synthetic strategies and physical properties. J Polym Sci A Polym Chem 48(2):251–284. https://doi.org/10.1002/pola.23755
15. Hoskins JN, Grayson SM (2009) Synthesis and Degradation Behavior of Cyclic Poly(ε-caprolactone). Macromolecules 42(17):6406–6413. https://doi.org/10.1021/ma9011076
16. Nasongkla N, Chen B, Macaraeg N, Fox ME, Fréchet JMJ, Szoka FC (2009) Dependence of Pharmacokinetics and Biodistribution on Polymer Architecture: Effect of Cyclic versus Linear Polymers. J Am Chem Soc 131(11):3842–3843. https://doi.org/10.1021/ja900062u
17. Chen B, Jerger K, Fréchet JM, Szoka FC (2009) The influence of polymer topology on pharmacokinetics: differences between cyclic and linear PEGylated poly(acrylic acid) comb polymers. J Control Release 140(3):203–209. https://doi.org/10.1016/j.jconrel.2009.05.021

Journal : SmallExtended 289	Article No : 3290	Pages : 21	MS Code : 3290	Dispatch : 1-7-2020

18. Chisholm MH, Gallucci JC, Yin H (2006) Cyclic esters and cyclodepsipeptides derived from lactide and 2,5-morpholinediones. Proc Natl Acad Sci U S A 103(42):15315–15320. https://doi.org/10.1073/pnas.0602662103
19. Zaldua N, Liénard R, Josse T, Zubitur M, Mugica A, Iturrospe A, Arbe A, De Winter J, Coulembier O, Müller AJ (2018) Influence of chain topology (cyclic versus linear) on the nucleation and isothermal crystallization of poly(l-lactide) and poly(d-lactide). Macromolecules 51(5):1718–1732. https://doi.org/10.1021/acs.macromol.7b02638
20. Stoclet G, Lefebvre JM, Séguéla R, Vanmansart C (2014) In-situ SAXS study of the plastic deformation behavior of polylactide upon cold-drawing. Polymer 55(7):1817–1828. https://doi.org/10.1016/j.polymer.2014.02.010
21. Dorgan JR, Williams JS, Lewis DN (1999) Melt rheology of poly(lactic acid): Entanglement and chain architecture effects. J Rheol 43(5):1141–1155. https://doi.org/10.1122/1.551041
22. Cooper-White JJ, Mackay ME (1999) Rheological properties of poly(lactides) AQ2 effect of molecular weight and temperature on the viscoelasticity of poly(l-lactic acid). J Polym Sci Part B Polym Phys 37(15):1803–1814. doi:10.1002/(SICI)1099–0488(19990801)37:15<1803:AID-POLB5>3.0.CO;2-M
23. Cendrowski-Guillaume SM, Le Gland G, Nierlich M, Ephritikhine M (2000) Lanthanide borohydrides as precursors to organometallic compounds. Mono(cyclooctatetraenyl) Neodymium Complexes. Organometallics 19(26):5654–5660. https://doi.org/10.1021/om000558f
24. Nakayama Y, Sasaki K, Watabane N (2009) Ring-opening polymerization of six-membered cyclic esters catalyzed by tetrahydroborate complexes of rare earth metals. Polymer 50(20):4788–4793. https://doi.org/10.1016/j.polymer.2009.08.024
25. Fischer EW, Sterzel HJ, Wegner G (1973) Investigation of the structure of solution grown crystals of lactide copolymers by means of chemical reactions. Kolloid-Z.u.Z. Polymere 251(1):980–990
26. Stoclet G, Seguela R, Lefebvre JM, Elkoun S, Vanmansart C (2010) Strain-induced molecular ordering in polylactide upon uniaxial stretching. Macromolecules 43(3):1488–1498. https://doi.org/10.1021/ma9024366
27. Yasuniwa M, Tsubakihara S, Sugimoto Y, Nakafuku C (2004) Thermal analysis of the double-melting behavior of poly(L-lactic acid). J Polym Sci Part B Polym Phys 42(1):25–32. https://doi.org/10.1002/polb.10674
28. Di Lorenzo ML (2006) Calorimetric analysis of the multiple melting behavior of poly(L-lactic acid). J Appl Polym Sci 100(4):3145–3151. https://doi.org/10.1002/app.23136
29. Pérez-Camargo RA, Mugica A, Zubitur M, Müller AJ (2017) Crystallization of cyclic polymers. In: Auriemma F, Alfonso GC, de Rosa C (eds) Polymer Crystallization I. Advances in polymer science, vol 276. Springer, Cham, pp 93–132
30. Rahman N, Kawai T, Matsuba G, Nishida K, Kanaya T, Watanabe H, Okamoto H, Kato M, Usuki A, Matsuda M, Nakajima K, Honma N (2009) Effect of polylactide stereocomplex on the crystallization behavior of poly(l-lactic acid). Macromolecules 42(13):4739–4745. https://doi.org/10.1021/ma900004d
31. Zhang J, Tashiro K, Tsuji H, Domb AJ (2008) Disorder-to-order phase transition and multiple melting behavior of poly(L-lactide) investigated by simultaneous measurements of WAXD and DSC. Macromolecules 41(4):1352–1357. https://doi.org/10.1021/ma0706071
32. Stoclet G, Seguela R, Lefebvre JM, Rochas C (2010) New insights on the strain-induced mesophase of poly(d, l-lactide): In situ WAXS and DSC study of the thermo-mechanical stability. Macromolecules 43(17):7228–7237. https://doi.org/10.1021/ma101430c
33. Roland CM, Archer LA, Mott PH, Sanchez-Reyes J (2004) Determining rouse relaxation times from the dynamic modulus of entangled polymers. J Rheol 48(2):395–403. https://doi.org/10.1122/1.1645516
34. Doi Y, Matsubara K, Ohta Y, Nakano T, Kawaguchi D, Takahashi Y, Kawagushi D, Takahashi Y, Takano A, Matsushita Y (2015) Melt rheology of ring polystyrenes with ultrahigh purity. Macromolecules 48(9):3140–3147. https://doi.org/10.1021/acs.macromol.5b00076
35. Wu S (1992) Predicting chain conformation and entanglement of polymers from chemical structure. Polym Eng Sci 32(12):823–830. https://doi.org/10.1002/pen.760321209
36. Joziasse CAP, Veenstra H, Grijpma DW, Pennings AJ (1996) On the chain stiffness of poly(lactide)s. Macromol Chem Phys 197(7):2219–2229. https://doi.org/10.1002/macp.1996.021970713
37. Grijpma DW, Penning JP, Pennings AJ (1994) Chain entanglement, mechanical properties and drawability of poly(lactide). Colloid Polym Sci 272(9):1068–1081. https://doi.org/10.1007/BF00652375

Journal : SmallExtended 289	Article No : 3290	Pages : 21	MS Code : 3290	Dispatch : 1-7-2020

38. Subramanian G, Shanbhag S (2008) Conformational properties of blends of cyclic and linear polymer melts. Phys Rev E Stat Nonlinear Soft Matter Phys. https://doi.org/10.1103/PhysRevE.77.011801
39. Lee E, Kim S, Jung YJ (2015) Slowing down of ring polymer diffusion caused by inter-ring threading. Macromol Rapid Commun 36(11):1115–1121. https://doi.org/10.1002/marc.201400713
40. Tsalikis DG, Mavrantzas VG (2014) Threading of ring poly(ethylene oxide) molecules by linear chains in the melt. ACS Macro Lett 3(8):763–766. https://doi.org/10.1021/mz5002096